Effect of Local Errors of Tipping-Bucket Rain Gauges on Rainfall-Runoff Simulations

Emad H. Habib, M.ASCE[1]; Ehab A. Meselhe, M.ASCE[2]; and Ananda V. Aduvala, S.M.ASCE[3]

Abstract: This study investigates the effect of local systematic and random errors of the commonly used tipping-bucket (TB) rain gauges on the accuracy of runoff predictions. A physically-based rainfall-runoff model is applied to analyze several storms in a humid midsize watershed in south Louisiana. Two types of systematic TB errors are considered, wind-induced losses and underestimation of high rainfall intensities due to the lack of gauge dynamic calibration. The effect of the TB errors is assessed by comparing hydrographs simulated using uncorrected and corrected rainfall input. The results indicate that wind and dynamic calibration effects can cause differences in estimating runoff volumes and peaks on the order of 5 to 15%. We also analyze the effect of random TB errors caused by the discrete gauge sampling mechanism. The computed runoff differences caused by the TB random errors were dependent on the magnitude of the runoff discharge, and on the temporal resolution of the rainfall input. However, the effect of random errors was found to be rather small, especially for large discharge.

DOI: 10.1061/(ASCE)1084-0699(2008)13:6(488)

CE Database subject headings: Rainfall; Runoff; Errors; Wind forces; Measurement; Simulation.

Introduction

Despite recent advances in rainfall remote sensing, rain gauge (RG) measurements continue to be the main source of surface rainfall information for both operational and research hydrologic studies. Many types of rain gauges are available, such as weighing bucket gauges, capacitance gauges, optical gauges, and tipping-bucket (TB) gauges. Over the recent years, TB rain gauges have become increasingly used by agencies such as the National Weather Service, the U.S. Geological Survey, the U.S. Army Corps of Engineers state districts, the National Park Service, and the U.S. Forrest Service.

Similar to several hydrological engineering applications, rainfall-runoff simulation models rely heavily on RG data as a source of rainfall information to provide flood predictions and forecasting, to issue flash flood warnings (Georgakakos 1996; Burn 1999; Doswell et al. 1999), and to analyze and design urban drainage systems (Schilling 1991; Zhu and Schilling 1996; Fankhauser 1997). In addition, rainfall-runoff predictions based on RG data are largely used as a reference against which the utility of more recent rainfall measuring techniques, such as radar or satellite, is assessed (Neary et al. 2004; Sun et al. 2000; Bedient et al. 2000).

Like all other field sensors, TB gauges are subject to errors. For rainfall-runoff modeling purposes, the most recognized limitation in using data from rain gauges is their limited near-point sampling and sparse spatial coverage. However, it is well recognized that RG data are also subject to other errors such as losses due to wind, wetting, evaporation, and splashing. The largest of these components is the wind-induced undercatch (Sevruk and Hamon 1984). Following Ciach (2003), we call these errors "local" to distinguish them from other errors related to insufficient spatial sampling. Another source of local TB gauge errors is due to dynamic calibration effects. TB gauges are typically calibrated by the manufacturer at a fixed rainfall rate that is typically low (few mm per h); however, such static calibration does not guarantee the conformance of the tipping-bucket size with the nominal calibration volume at high rainfall rates. Due to the measurement principle of the TB gauges, some of the incident rainfall is missed between successive tips of the bucket, which results in an underestimation of actual rainfall volumes and intensities. This underestimation is negligible at small rainfall rates, but grows nonlinearly with the increase of rainfall rates (Niemczynowicz 1986; Humphrey et al. 1997; Luyckx and Berlamont 2001).

Besides these systematic errors, TB measurements are also associated with local random errors (Fankhauser 1997; Yu et al. 1997; Nystuen and Proni 1996). These errors are mainly related to the discrete sampling mechanism of the TB gauge and are caused by uncertainties in defining start and end of rain event, partial filling of the bucket, and instabilities in the water inflow into the collecting funnel. Ciach (2003) and Habib et al. (2001) showed that such random errors have significant magnitudes, mainly at small rainfall intensities and short time scales.

While the effect of limited RG spatial sampling on the predictions of rainfall-runoff models has been the subject of numerous studies (Krajewski et al. 1991; Chaubey et al. 1999), the effect of local systematic and random errors discussed above has not been

[1]Assistant Professor, Dept. of Civil Engineering and Center for Louisiana Water Studies, Univ. of Louisiana at Lafayette, P.O. Box 42291, Lafayette, LA 70504-2291. E-mail: habib@louisiana.edu

[2]Professor, Dept. of Civil Engineering and Center for Louisiana Water Studies, Univ. of Louisiana at Lafayette, P.O. Box 42291, Lafayette, LA 70504-2291. E-mail: meselhe@louisiana.edu

[3] BPC Group Inc., 6925 Lake Ellenor Dr., Suite 112, Orlando, FL 32809; formerly, Graduate Research Assistant, Dept. of Civil Engineering, Univ. of Louisiana at Lafayette, P.O. Box 42291, Lafayette, LA 70504-2291. E-mail: anandvishnu@louisiana.edu

Note. Discussion open until November 1, 2008. Separate discussions must be submitted for individual papers. To extend the closing date by one month, a written request must be filed with the ASCE Managing Editor. The manuscript for this paper was submitted for review and possible publication on July 10, 2006; approved on October 9, 2007. This paper is part of the ***Journal of Hydrologic Engineering***, Vol. 13, No. 6, June 1, 2008. ©ASCE, ISSN 1084-0699/2008/6-488–496/$25.00.

Downloaded 26 Nov 2008 to 128.255.27.170. Redistribution subject to ASCE license or copyright; see http://pubs.asce.org/copyright

addressed as extensively. Earlier studies by Giuliani et al. (1996), Fankhauser (1997), and Yu et al. (1997) analyzed the effect of some of these local errors on the simulation of storm sewer flows. However, their studies were mostly based on hypothetical rainfall/flow data and on rather simplified runoff prediction models. In the present study, we focus on the effect of the most significant components of the local systematic TB gauge errors: Wind-induced undercatch and dynamic calibration effects. We also analyze the effect of the random errors and see how they propagate into the hydrologic model predictions. Recognizing recent advances in rainfall-runoff models, we use a process-based distributed hydrologic model to simulate several runoff events recorded in a midsize watershed in south Louisiana. The effect of TB systematic errors is analyzed by comparison of runoff hydrographs obtained with and without applying correction factors to the recorded TB rainfall records. An empirical model is implemented through a Monte Carlo simulation experiment to simulate the TB random error and assess its effect on the simulated hydrographs. The magnitudes of systematic errors in TB measurements are expected to vary according to the temporal resolution of TB data at which the correction factors are estimated and applied. Similarly, according to Ciach (2003) and Habib et al. (2001), TB random errors are reduced as rainfall records are averaged to coarser resolutions. Therefore, three time scales of 5 min, 15 min, and 1 h are considered in this analysis. These time scales are of relevance to rainfall-runoff applications, especially in midsize catchments.

This paper is organized as follows. First, we describe the study watershed and the available rainfall-runoff data. We then briefly introduce the hydrologic model used to perform the rainfall-runoff simulations. Next, methods used to simulate the local systematic and random TB errors are described. The effect of TB errors on runoff simulations is characterized in terms of their impact on predicting runoff volumes and peaks. We close with concluding remarks on the practical implications of this analysis for hydrologic modeling studies.

Study Site and Experimental Data

The site of this study is the 35 km^2 Isaac Verot (IV) watershed located in the city of Lafayette in south Louisiana (Fig. 1). The watershed is a subdrainage area of the Vermilion river basin, which drains into the Gulf of Mexico. The IV watershed is a typical low-gradient watershed where open channel flow plays a vital role in runoff production (Habib and Meselhe 2006). The terrain elevation in the watershed, with reference to mean sea level, ranges from approximately 6 m near the outlet to 11.5 m at the catchment divide. The main channel in the watershed has a slope of 0.0008. An approximate estimate of the concentration time of this low-gradient watershed was found to be in the order of a few h. The watershed is frequently subject to frontal systems, air-mass thunderstorms, as well as tropical cyclones with annual rainfall of about 140 to 155 cm and monthly accumulations as high as 17 cm (6.6 in.). There are basically two main soil types in the IV watershed: Coteau frost soil and Memphis frost soil. Both soils are texturally classified as silt loam with low- to medium-drainage capacity. The land use in the watershed is composed of urban areas, cropland, pasture, and some forest areas.

The Department of Civil Engineering at the University of Louisiana at Lafayette has deployed a dense experimental network of rainfall and runoff monitoring sites over the watershed (Fig. 1). A total of 13 tipping-bucket rain gauge sites are distributed over the watershed and every site has a dual-gauge setup for improved data continuity and quality (Krajewski et al. 2003). The gauges have an orifice size of 30.5 cm (12 in.) and are equipped with a digital data logger that records the time of occurrence of successive 0.254 mm (0.01 in.) tips, which can be used to construct a time series of rainfall intensities at any desired time scale (e.g., few minutes or hourly). Streamflow measurements are collected at the outlet of the watershed, as well as at four interior locations using bidirectional acoustic (side looking) velocity meters, from which discharge estimates can be obtained. In this study, discharge information at the outlet of the watershed only is used to calibrate and validate the hydrologic model. Five-minute wind speed measurements are also collected using a total weather station located at the northern boundary of the watershed.

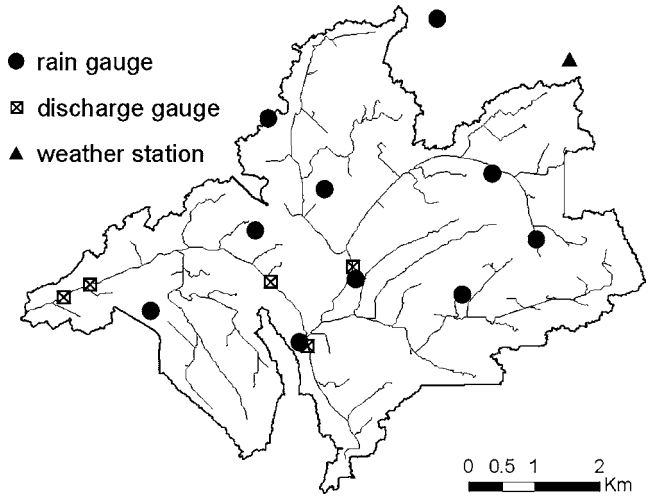

Fig. 1. Isaac Verot (IV) experimental watershed in south Louisiana. Different symbols indicate the locations of hydrological and meteorological monitoring stations.

Rainfall-runoff records have been continuously collected in the IV watershed since 2003. In this study, a total of 18 significant rainfall-runoff events are considered (Table 1). It should be noted that these events were grouped into five simulation periods, where each period was simulated in a continuous mode. The selected runoff events were caused by both localized and large-scale heavy rainfall storms. The events include tropical storm Matthew, which made landfall in south Louisiana on October 10, 2004. Durations of the events ranged from a few hours to a few days. An extensively wet period of 20 days was also included in the analysis. Event-total rainfall volumes were in the range of 30 to 100 mm with four events exceeding 200 mm. A total of 283 mm of rainfall was observed during tropical storm Matthew over the course of 3 days. Maximum 5-min average rainfall intensities exceeded 100 mm/h during four storms, with most storms in the range of 12 mm/h to 100 mm/h. Significant runoff volumes and peaks were observed at the outlet of the IV watershed during most of these rainfall storms. Runoff-rainfall ratios were in the range of 20 to 35% with several storms exceeding 60%. Most discharge peaks were less than 40 m^3/s, three peaks exceeded 50 m^3/s, and the maximum observed peak was 61.8 m^3/s (equivalent to a unit peak of 1.8 $m^3/s/km^2$). Five-minute average wind speed observations collected with the total weather station were mostly in the range of 3 to 5 m/s. No significant correlation was found between wind speed and rainfall rates recorded during the events.

Downloaded 26 Nov 2008 to 128.255.27.170. Redistribution subject to ASCE license or copyright; see http://pubs.asce.org/copyright

Table 1. Summary of Rainfall-Runoff Events during the Five Continuous Simulation Periods

Simulation period	Event	Total rainfall volume (mm)	Runoff/rainfall ratio (%)	5 min maximum rainfall intensity (mm/hr)	Maximum runoff Peak (m^3/s)	Maximum wind speed (m/s)
1	9/9/2003–9/13/2003	112	31.0	94.5	14.9	3.8
	9/21/2003–9/23/2003	54	30.3	70.1	14.0	2.7
	10/9/2003–10/11/2003	83	60.8	30.5	39.6	2.9
	11/18/2003–11/24/2003	205	56.0	94.5	50.5	5.1
	12/8/2003–12/13/2003	31	27.5	45.7	8.7	3.9
	12/23/2003–12/29/2003	31	4.6	36.6	8.3	3.4
2	1/4/2004–1/9/2004	52	22.0	54.9	7.3	5.1
	1/17/2004–1/17/2004	8	79.2	12.2	6.6	3.0
	1/24/2004–2/14/2004	188	21.7	85.3	9.9	4.5
	2/23/2004–2/26/2004	49	27.0	57.9	9.1	4.2
3	4/24/2004–4/25/2004	85	69.4	116.5	41.9	4.8
	4/30/2004–5/1/2004	62	43.6	55.7	14.3	4.0
	5/11/2004–5/18/2004	216	60.9	103.6	40.0	4.2
4	6/5/2004–6/5/2004	34	33.4	90.8	12.8	5.2
	6/13/2004–6/16/2004	32	35.4	51.5	8.2	3.6
	6/22/2004–6/29/2004	281	58.9	130.4	61.8	4.0
	7/6/2004–7/7/2004	31	13.9	70.6	3.6	4.3
5	10/7/2004–10/10/2004	283	67.9	134.6	54.4	3.7

Rainfall-Runoff Model

In the current study, the gridded surface subsurface hydrologic analysis (GSSHA) system is used to develop a rainfall-runoff model for the IV watershed. GSSHA is a fully distributed parameter, process-based hydrologic model. It uses finite difference and finite volume methods to simulate different hydrologic processes, such as rainfall distribution and interception, overland water retention, infiltration, evapotranspiration, two-dimensional overland flow, and one-dimensional channel routing. GSSHA also provides a detailed modeling of the soil moisture profile in the unsaturated zone using different methods such as Green and Ampt and Richards' equation. A full description of GSSHA can be found in Downer and Ogden (2002, 2004).

The model setup adopted in this study included the following options: Two-dimensional diffusive wave approximation of the de Saint Venant equations for overland flow, one-dimensional explicit diffusive wave method for channel flow, Penman-Monteith equation for evapotranspiration calculations (Monteith 1965), and the Green and Ampt infiltration with redistribution (GAR) method (Ogden and Saghafian 1997) for flow simulation in the unsaturated zone. The GAR method includes soil moisture accounting, which simulates the soil moisture redistribution along the soil profile during a runoff event, as well as the change in soil moisture due to evapotranspiration between rainfall events. Therefore, it was possible to simulate each of the five multiple-event simulation periods (Table 1) in a continuous mode. Accordingly, model soil moisture initial conditions have to be specified only at the beginning of each simulation period. The effect of these assumed initial conditions was very minimal especially that the durations of the simulation periods were fairly long. Nevertheless, to avoid any possible effects, the model simulations were started at earlier times and the first hydrograph in each period was not included in any further analysis.

The watershed topographic and hydrologic properties are represented using a square 100×100 m^2 Cartesian grid. Topographic information for the watershed was obtained from recent high-resolution LIDAR data for the state of Louisiana (Craig and Philips 2003). Channel dimensions were compiled from historical surveys and were checked and updated by conducting recent surveying measurements in 2004. Overland hydraulic properties (e.g., roughness parameters) are assigned at each grid pixel based on land use information. Soil hydraulic parameters necessary for the GAR method (e.g., saturated hydraulic conductivity, soil suction head, effective porosity), and evapotranspiration parameters (e.g., vegetation transmission coefficients and root depths) were assigned based on spatial variations in the combined classifications of soil type and land use maps. Initial values of these parameters are selected based on literature sources and will be adjusted through a model calibration procedure as described later.

Methods of Error Simulation

To examine the effects of different local RG errors on runoff predictions, we follow a simple comparative approach where model simulations are performed using different sets of rainfall input. For systematic rainfall errors, the rainfall-runoff model will be forced using both uncorrected and corrected rainfall measurements. The corrections will be based on estimates of local errors due to wind and dynamic calibration effects. For local random errors, a Monte Carlo random simulation approach is followed. Several realizations of RG rainfall observations will be generated by contaminating the actual RG measurements with random errors that have certain variance structure. The different RG realizations are then used to drive the rainfall-runoff model and to assess the distribution of uncertainties in the resulting runoff predictions. In the following, we describe the methods followed to correct for the RG systematic errors and to statistically simulate the random errors.

Downloaded 26 Nov 2008 to 128.255.27.170. Redistribution subject to ASCE license or copyright; see http://pubs.asce.org/copyright

Wind-Induced Error

Undercatchment in RG measurements due to wind effect has been the subject of numerous studies [see Sevruk and Hamon (1984) and Sevruk and Lapin (1993) for a detailed review]. Wind effect correction methods can be classified into two main approaches: Field intercomparison studies and numerical modeling simulations. In the first approach, observations from gauges elevated above the ground are compared to those from ground level pit gauges (Legates and Deliberty 1993; Yang et al. 1998) and empirical formulas are developed to estimate correction factors as a function of wind speed. In the second and more recent approach, computational fluid dynamics techniques are applied to simulate the wind flow field around the gauge geometry and to track the trajectories of rain droplets as they approach the gauge orifice. Following this approach, Nespor and Sevruk (1999) developed approximate formulas to estimate wind-induced errors as a function of wind velocity, rainfall intensity, and raindrop size distribution. The importance of including raindrop size distribution information to correct for wind-related errors has been recently emphasized by both numerical (Habib et al. 1999) and field (Duchon and Essenberg 2001) studies. However, such information is not typically available for most operational applications. Therefore, in the current study, we use an empirical correction formula developed by Yang et al. (1998) for the National Weather Service standard precipitation gauges

$$R_{\text{corrected}} = R_{\text{measured}}[100 \exp(-4.606 + 0.041\, u^{0.69})] \quad (1)$$

The expression in the brackets represents a correction factor that depends solely on the wind speed (u in m/s) that is associated with the measured rainfall intensity R. It should be noted that the above formula was developed for corrections of daily rainfall accumulations. However, as illustrated in Habib et al. (1999), this formula compared reasonably well with other more accurate formulas when applied at finer time scales (few minutes). It is also noted that while this formula was developed for a gauge type different from the gauges in the IV watershed, it is still reasonable to be used in the current analysis since the focus is not on actual corrections of rainfall measurements. Instead, the formula is used to illustrate the impact of wind effects on RG measurements and the subsequent impact on the accuracy of runoff predictions. We also note that errors obtained using the formula of Yang et al. (1998) were in the same order of magnitude of errors that were obtained by Duchon and Essenberg (2001) in their analysis of field measurements with the same TB gauge model used in our study.

Errors due to Lack of Dynamic Calibration

To investigate the effect of lack of gauge dynamic calibration, we implemented a laboratory procedure described in Humphrey et al. (1997) to dynamically calibrate the TB rain gauges located in the watershed. In this procedure, a programmable pump is used to apply a prespecified series of different flow rates. The RG is connected to a computer through a data logger to record the number and timing of the occurrence of each tip. Recorded tip information is used to estimate RG rainfall rates, which are then compared against the corresponding true pump rates. As expected, TB gauges suffer from a significant underestimation, which increases nonlinearly as the rainfall intensity increases. A correction formula of the following form was developed for each calibrated rain gauge:

$$R_{\text{corrected}} = C_1 R_{\text{measured}} + C_2 R^2_{\text{measured}} \quad (2)$$

where C_1 and C_2=fitting coefficients. The values of these two coefficients obtained for different gauges in the IV watershed ranged from 0.99 to 1.04 for C_1 and from 0.0006 to 0.0008 for C_2 (with R expressed in mm/h). Note that unlike the wind correction formula, the dynamic calibration correction is dependent on the magnitude of the recorded RG rainfall intensity.

Local Random Error

In an effort to statistically characterize the RG local random errors, Habib et al. (2001) used a data-driven simulation model of the RG sampling mechanism and its measurements. They developed approximate formulas to describe the error dependence on the time resolution of rainfall measurements and on the RG volume and temporal sampling resolution. In a recent study, Ciach (2003) designed a field experiment to compare measurements from a cluster of collocated 15 rain gauges that were deployed over an area of about 8 m$\times$8 m. Ciach (2003) developed a simple analytical model of the RG local random error, which can be used to obtain estimates of the standard deviation of the error at any given time scale and rainfall intensity. Through a Monte Carlo experiment, we will apply this model to simulate different realizations of the RG local random error and analyze its effect on the accuracy of runoff predictions. Full details of this model are available in Ciach (2003) and only a brief description is given here. A main assumption behind the model is that averaging the measurements of the 15 collocated gauges provides a reasonable approximation of the true point rainfall. The local random error (e_T) can then be defined as the relative difference between the rain gauge measurement ($R_{g,T}$) and the corresponding true point rainfall (R_T) at any given time scale (T) of the available rainfall measurements

$$e_T = \frac{R_{g,T} - R_T}{R_T} \quad (3)$$

This definition explicitly accounts for the experimentally observed dependence of the error on both R and T. While Eq. (3) implies that the mean of the error is always zero, the standard deviation of the error (σ_g) depends on both R and T. Ciach (2003) analyzed the collocated 15 gauge measurements and used nonparametric regression to estimate σ_g as follows:

$$\sigma_g(T,R) = \alpha(T) + \frac{\beta(T)}{R_T} \quad (4)$$

The dependence of the model parameters α and β on the time scale (T) was approximated using a nonlinear minimization procedure [see Fig. 6 in Ciach (2003)].

Eq. (4) provides a convenient tool to simulate RG uncertainties due to the effect of local random errors for any given RG temporal resolution. However, due to the lack of information on true rainfall rates (R_T), we will hypothetically consider the actual rain gauge observations as "true" measurements of point rainfall and use them to generate other sets of rainfall inputs contaminated with RG random errors. The simulation procedure is described as follows. Consider a time series of "true" rainfall measurements with a certain resolution T. At each time step in the series, σ_g is computed using Eq. (4) with the parameters α and β selected according to T. We then generate normally distributed random values of e_T with a mean of zero and a standard deviation σ_g. The generated e_T values are substituted into Eq. (3) to estimate realizations of the RG rainfall intensity ($R_{g,T}$). This proce-

Downloaded 26 Nov 2008 to 128.255.27.170. Redistribution subject to ASCE license or copyright; see http://pubs.asce.org/copyright

Table 2. Statistical Assessment of Model Prediction Errors during Calibration (September–October 2003) and Validation (April–May 2004; October 2004) Events. Some Events Contained More Than One Peak. The Corresponding Errors due to Wind Effect and Lack of Dynamic Calibration Estimated on 5 min Resolution Rainfall Data are Also Included.

		Difference in runoff volume V_d (%)			Difference in runoff peak P_d (%)	
Event	Model error in predicting runoff volume (%)[a]	Dynamic calibration	Wind induced	Model error in predicting runoff peak (%)[a]	Dynamic calibration	Wind induced
9/9/2003–9/13/2003[b]	6.1	7.2	12.3	0.2	8.6	11.1
				21.6	6.9	13.7
9/21/2003–9/23/2003	21.3	5.6	8.2	−0.4	5.4	6.5
10/9/2003–10/11/2003	−0.7	4.2	7.6	−6.9	2.9	6.0
4/24/2004–4/25/2004	27.1	6.3	9.8	22.6	3.8	6.3
4/30/2004–5/1/2004[b]	8.9	5.1	10.5	26.2	5.9	12.1
				2.3	4.7	9.6
5/11/2004–5/18/2004	−2.6	4.9	9.2	−6.2	3.6	5.9
10/7/2004–10/10/2004[b]	10.3	4.7	8.1	10.3	1.0	1.6
				−4.3	4.6	7.3

[a]Model errors are calculated as relative difference between observed and simulated discharge values [formulas similar to Eqs. (5) and (6)].
[b]Events containing two runoff peaks.

dure is repeated at every time step to produce multiple realizations of the time series measurements of each rain gauge in the watershed. Each generated time series can be used as an input into the GSSHA model to study the impact of RG local random errors on the simulated hydrographs.

Results

Model Calibration and Validation

Prior to using the GSSHA model to assess effects of RG local errors, we performed calibration and validation analyses using the split-sample test method (Klemes 1986). One set of rainfall-runoff events was used to calibrate the model while other events were reserved for validation (Table 2). Some of the recorded events (Table 1) had missing discharge measurements and, therefore, were not included in the validation simulations. All simulations, which included rainy and dry periods, were performed in a continuous mode. Model calibration was designed to minimize overall differences between observed and simulated runoff hydrographs. The main model parameters adjusted during calibration included soil infiltration parameters and overland and channel roughness coefficients. However, the simulated runoff peaks and volumes were most sensitive to changes in the soil saturated hydraulic conductivity and to a lesser degree to the roughness coefficients. Examples of calibration and validation results are shown in Fig. 2. A quantitative assessment of results is given in Table 2 in terms of runoff volume and peak errors computed by assessing differences between simulated and observed discharge values. We consider the calibration results acceptable, given that the main focus of this study is not on the model development itself, and that the model will be used to assess the sensitivity of runoff prediction to RG local errors.

Effect of Local Systematic Errors

To examine the effect of local gauge errors on runoff prediction, two sets of rainfall input are considered: Measured (uncorrected) rainfall rates and rainfall rates after correction for wind-induced errors and lack of dynamic calibration. Each correction is applied separately to the rainfall measurements at three different rainfall resolutions: 5 min, 15 min, and 1 h. For each rainfall input, the calibrated GSSHA model is used to predict runoff at the watershed outlet. Runoff volumes and peaks predicted using the uncorrected rainfall input are compared against those obtained after correcting for each error source. Differences in predictions are quantified using the following statistics:

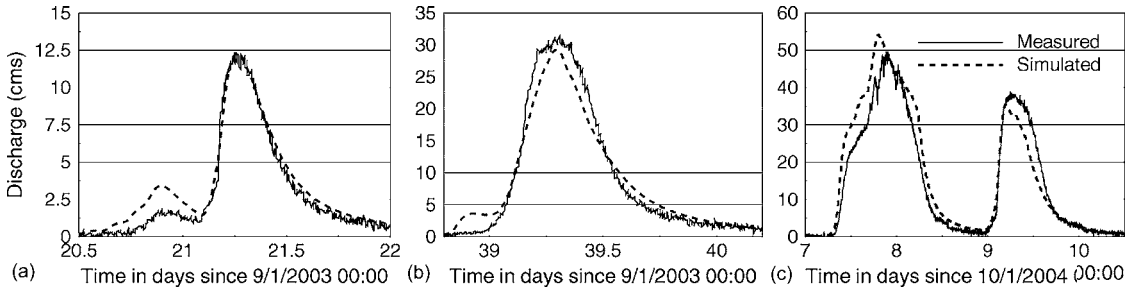

Fig. 2. Examples of simulated hydrographs using the GSSHA model during calibration (a, b) and validation (c) events. Calibration and validation simulation runs are driven by rainfall data from the 30 rain gauges in the IV watershed.

Downloaded 26 Nov 2008 to 128.255.27.170. Redistribution subject to ASCE license or copyright; see http://pubs.asce.org/copyright

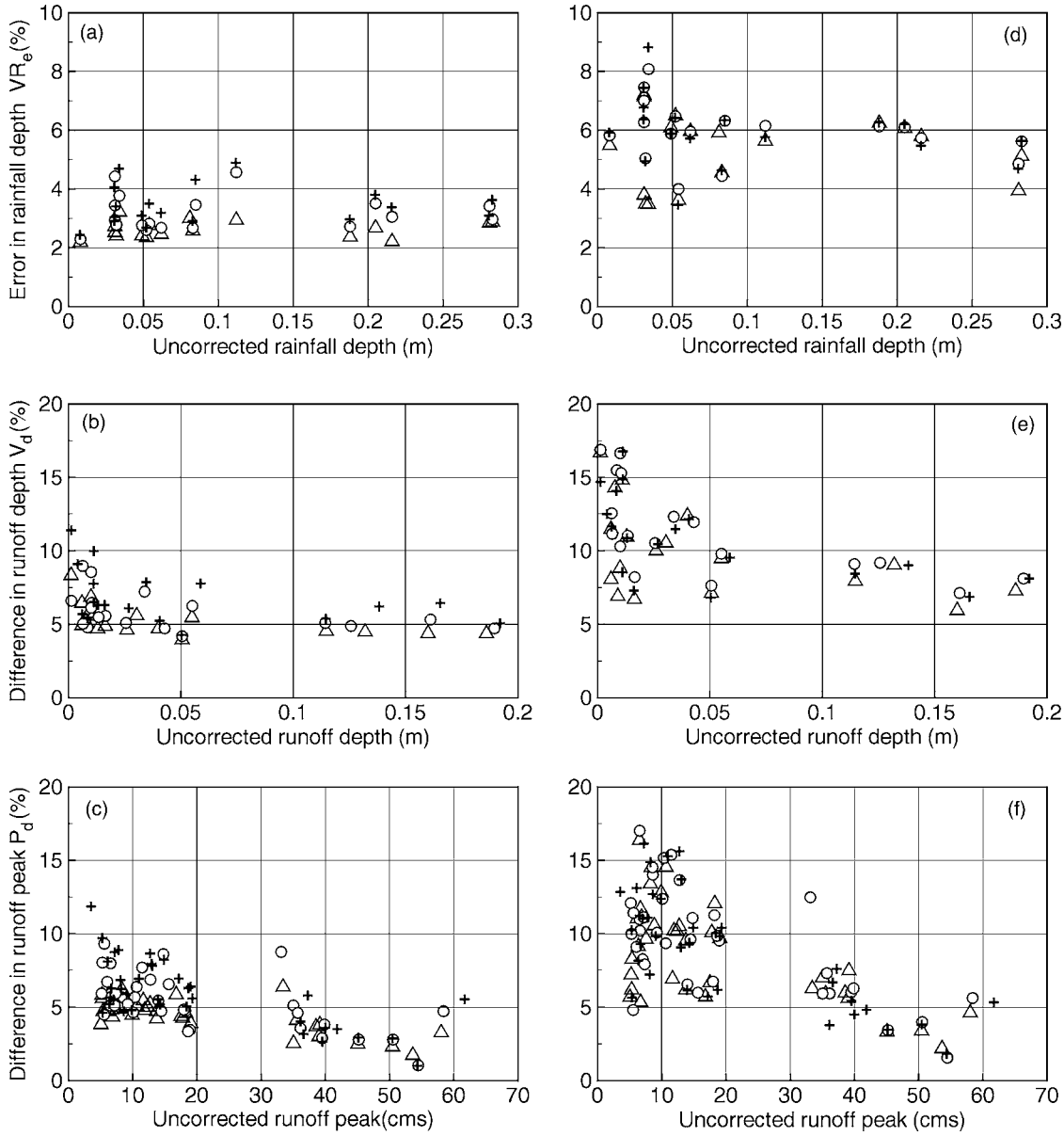

Fig. 3. Effect of lack of dynamic calibration (a, b, c) and wind undercatch (d, e, f) on rainfall volumes (a, d), and on prediction accuracy of runoff volumes (b, e) and peaks (c, f). Different symbols correspond to different rainfall data resolutions: 5 min (plus), 15 min (circle), and 1 h (triangle).

$$V_d(\%) = \frac{V_c - V_u}{V_u} 100 \tag{5}$$

$$P_d(\%) = \frac{P_c - P_u}{P_u} 100 \tag{6}$$

where V_u=runoff volume obtained with uncorrected rainfall input, and V_c=corresponding volume obtained using the corrected rainfall input after adjustment due to either wind effect or dynamic calibration, and V_d=difference in runoff volume after correcting the rainfall input (%). Similarly, P_u and P_c=runoff peaks obtained using the uncorrected and corrected rainfall inputs, respectively, and P_d represents the difference in runoff peak (%).

To relate uncertainties in the rain gauge measurements to the effect on runoff predictions, a similar statistical measure is computed for rainfall

$$\mathrm{VR}_e(\%) = \frac{\mathrm{VR}_c - \mathrm{VR}_u}{D_u} 100 \tag{7}$$

where VR_u and VR_c=volumes of uncorrected and corrected rainfall input in each event, respectively, and VR_e=corresponding rainfall volume error (%).

VR_e, V_d, and P_d are computed for each of the 18 rainfall-runoff events within the main five simulation periods and the results are summarized in Fig. 3 for both sources of rainfall errors and for the three considered correction temporal scales. Consider first the error in rainfall volume. Errors in quantifying rainfall volumes are due to lack of dynamic calibration and wind effect and are in the range of 2 to 5% and 3 to 9%, respectively [Figs. 3(a and d)]. These errors propagated into the model simulations and resulted in enhanced runoff volume differences [Figs. 3(b and e)]. Runoff volume differences due to lack of dynamic calibration range from 4 to 10%. The corresponding differences caused by

Downloaded 26 Nov 2008 to 128.255.27.170. Redistribution subject to ASCE license or copyright; see http://pubs.asce.org/copyright

wind effect were higher with a range of 6 to 18%. Note that events with smaller rainfall-runoff volumes are more sensitive to the applied rainfall corrections. Runoff peaks were also affected by both sources of RG errors [Figs. 3(c and f)]. Peak differences in the range of 2–12% and 2–18% are noticed for the cases of dynamic effects and wind effects, respectively. It is also noticed that relatively high peaks (30 m^3/s or higher) are less affected by TB rainfall errors.

Now consider the effect of applying corrections at different temporal resolutions of the rainfall input (see different symbols in Fig. 3). For dynamic calibration effects, it is noticed that rainfall and runoff differences are reduced when the corrections are applied at coarser scales (e.g., 1 h versus 5 min). For example, at an hourly scale, the estimated differences in both runoff volumes and peaks are significantly small ($V_d < 8\%$ and $P_d < 6\%$) in comparison to the corresponding values at a 5 min scale. This is explained by the fact that as high-intensity rainfall values are smoothed at coarse resolutions, the correction factors estimated by Eq. (2) are significantly underestimated, and as such, their effect on predicting runoff volumes and peaks is diminished as well. As expected, the effect of rainfall smoothing is more noticeable for large runoff peaks than for small ones. Considering the wind effect, it is first noted that the wind correction factor in Eq. (1) depends only on the wind speed, which is obtained by averaging wind measurements to the correction scale under consideration. Analysis of the distributions of wind speeds at the three time scales (not shown here) indicated that, unlike rainfall, large wind speeds remain relatively sustained when averaged from 5 min to longer durations. Therefore, unlike the case of dynamic calibration effects, the estimated wind correction factors and their effect on runoff predictions did not decrease with coarsening of the correction time scale.

To provide better assessment of the impact of RG errors on the rainfall-runoff modeling results, the estimated differences in predicted runoff volumes and peaks should be relatively compared to other sources of errors that affect the model results. These other possible errors, typically caused by data limitations and parameter estimation, usually manifest themselves as differences between observed and simulated runoff discharges during the calibration and validation tests. Table 2 shows a comparison of runoff differences caused by RG errors (due to wind and dynamic effects), versus model errors obtained during the calibration and validation events. For most of the simulated events, runoff differences due to RG errors were comparable to the model calibration and validation errors. Implications of this result for modeling practices are discussed in the summary and discussions section.

Effect of Local Random Errors

The random error model described above [Eqs. (3) and (4)] was applied to generate 500 realizations of RG measurements. Each realization was used to run the rainfall-runoff model to produce the corresponding 500 runoff realizations. Due to computational considerations, this analysis was performed on only one simulation period (October 2004). Similar to the cases of systematic errors, we considered three time scales of the rainfall input. To quantify the impact on runoff predictions, the following statistical uncertainty range (UR) measure was computed at each time step within the simulation period:

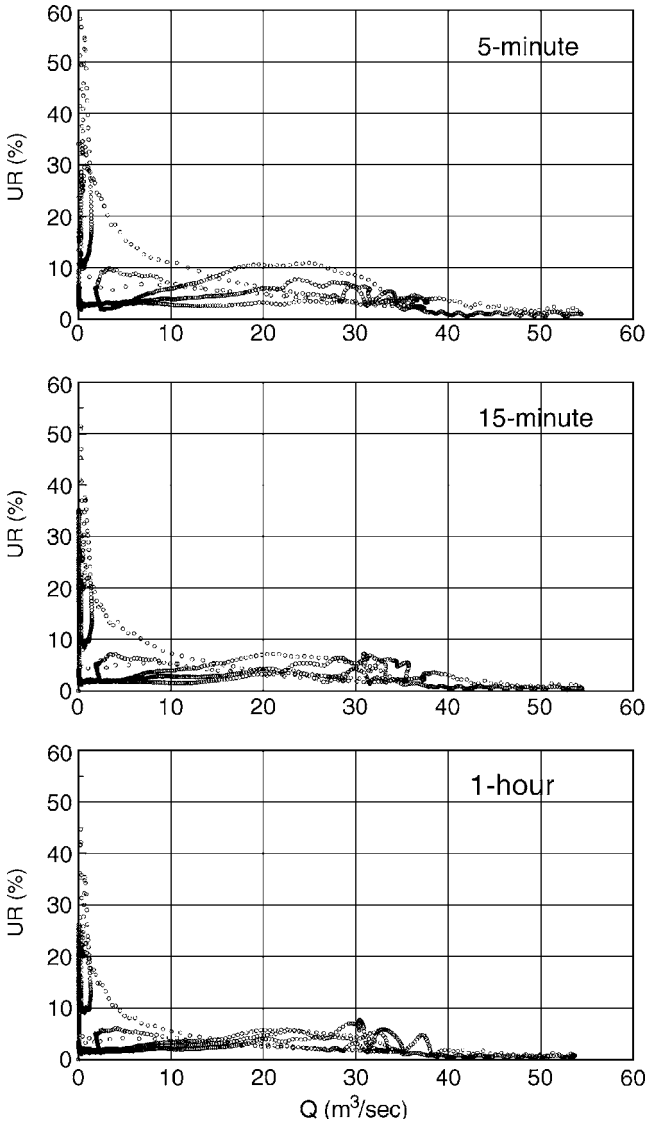

Fig. 4. UR of the predicted runoff discharges caused by TB random errors during the October 2004 simulation period for three rainfall resolutions

$$\mathrm{UR}_i = \frac{(P_{97.5,i} - P_{2.5,i})}{Q_i} 100 \tag{8}$$

where $P_{2.5,i}$ and $P_{97.5,i}$=2.5 and 97.5 percentiles of the discharge predictions, respectively, computed from the distribution of the 500 simulations at each time step i, and Q_i=model discharge prediction obtained using the "true" rainfall measurements. UR provides a quantitative measure of the degree of uncertainty in the model predictions due to the RG local random errors. The computed UR factors are plotted versus the corresponding Q values for each time resolution (Fig. 4). As expected, and due to the dependence of the error variance on the magnitude of rainfall intensities [Eq. (4)], the local random errors had more impact on low rainfall intensities. For small Q values (<5 m^3/s), RG random errors cause significant uncertainties as high as 40–80%. However, for medium to high discharge values, the uncertainty decreases significantly and does not exceed 10–12%. For higher discharge peaks, the effect of the RG random errors becomes negligible. Finally, comparison of UR values obtained at the three analyzed time scales indicates that the impact of local random

Downloaded 26 Nov 2008 to 128.255.27.170. Redistribution subject to ASCE license or copyright; see http://pubs.asce.org/copyright

errors is more important when high-resolution rainfall measurements are used to drive hydrologic predictions.

Summary and Discussions

In this study, we explored the impact of three types of tipping-bucket rain gauge measurement errors on the accuracy of runoff predictions. The examined errors are caused by wind undercatch, calibration-related errors due to dynamic effects of water flow into the gauge buckets, and local random errors due to the discrete sampling mechanism of the rain gauge. The impact of these errors was assessed in terms of their effect on predicting runoff volumes and discharge peaks. The results showed that dynamic calibration and wind effects can cause differences in estimating runoff volumes in the range of 4 to 10% and 6 to 18%, respectively. The impact on predicting runoff peaks was also significant (2 to 12% for dynamic calibration effect, and 2 to 18% for wind effect). The error correction factors were underestimated when RG measurements are used at coarse resolutions (e.g., 1 h), especially for the case of dynamic calibration effects. It was also noted that, due to the inherent nonlinearity in the rainfall-runoff transformation, RG-induced errors got enhanced as they propagated into the hydrologic simulations. Finally, a Monte Carlo simulation experiment was applied to investigate the impact of RG local random errors. Random errors and the corresponding uncertainty in runoff simulations are more significant when high-resolution rainfall measurements are used to drive hydrologic predictions. However, the effect was found to be rather small ($<10\%$), especially for large discharge values.

The results of this study should be considered within the context of the specific rainfall-runoff model application. The magnitude of the estimated differences in runoff predictions due to gauge local errors can be significant for studies that focus on accurate flood peak estimation. Differences in predicting runoff volumes, even as small as 5–10%, also may not be negligible, especially for applications that are concerned with water-budget analyses. We note that this study was based on analysis of a relatively midsize watershed (35 km^2). Therefore, further analysis might be required to examine the effect and significance of local gauge errors on runoff simulations across different watershed scales (i.e., from small- to large-size watersheds).

The estimated differences in runoff predictions should be interpreted in a relative sense with respect to other sources of modeling errors. The effect of local RG errors on runoff predictions might be overshadowed by other error sources, such as limited rainfall sampling, lack of necessary calibration data, imperfect model structure, and uncertainties associated with parameter estimation. In the present study, differences in the predicted runoff volumes and peaks due to gauge errors were significant in the sense of being of a similar magnitude to model errors obtained during calibration and validation tests. However, this may not be the case in other applications, where poor input or calibration data can dominate the model prediction uncertainty. However, given the recent advances in hydrologic modeling techniques, and with the increasing availability of high-resolution hydrological and hydrometeorological data, it becomes relevant to quantify all possible sources of errors, including those that are often overlooked, such as the RG local measurement errors, and account for their contribution to the overall model uncertainty.

Based on the results obtained herein, some practical recommendations can be made regarding the use of tipping-bucket rain gauges for rainfall-runoff modeling applications. Whenever possible, measurements of wind speeds should be collected and used to adjust rainfall input data. Although dynamic calibration of tipping-bucket rain gauges might be laborious and time consuming, it might be warranted especially in applications that use rainfall data with high temporal resolutions. While it can be argued that most of the errors examined in this study can be compensated for through the model calibration procedure, this might result in unjustified adjustments to the model parameters. Instead, operational efforts should be dedicated towards adjusting for these error sources as a part of collecting and preprocessing the rain gauge data.

References

Bedient, P. B., Hoblit, B. C., Gladwell, D. C., and Vieux, B. E. (2000). "NEXRAD radar for flood prediction in Houston." *J. Hydrol. Eng.*, 5(3), 269–277.

Burn, D. H. (1999). "Perceptions of flood risk: A case study of the Red River flood of 1997." *Water Resour. Res.*, 35(11), 3451–3459.

Chaubey, I., Haan, C. T., Salisbury, J. M., and Grunwald, S. (1999). "Quantifying model output uncertainty due to spatial variability of rainfall." *J. Am. Water Resour. Assoc.*, 38(5), 1113–1123.

Ciach, G. J. (2003). "Local random errors in tipping-bucket rain gauge measurements." *J. Atmos. Ocean. Technol.*, 20, 752–759.

Craig, J., and Philips, H. (2003). "LIDAR technical workflow." 3001 Inc., Gainesville, Fla.

Doswell, C. A. III, Brooks, H. E., and Maddox, R. A. (1999). "Flash flood forecasting: An ingredients-based methodology." *Weather Forecast.*, 11, 560–581.

Downer, C. W., and Ogden, F. L. (2002). "GSSHA user's manual, gridded surface subsurface hydrologic analysis, Vers. 1.43 for WMS 6.1." *Engineer Research and Development Center Technical Rep.*, Vicksburg, Miss.

Downer, C. W., and Ogden, F. L. (2004). "GSSHA: Model to simulate diverse stream flow producing processes." *J. Hydrol. Eng.*, 9(3), 161–174.

Duchon, C. E., and Essenberg, G. R. (2001). "Comparative rainfall observations from pit and aboveground rain gauges with and without wind shields." *Water Resour. Res.*, 37, 3253–3263.

Fankhauser, R. (1997). "Measurement properties of tipping bucket rain gauges and their influence on urban runoff simulation." *Water Sci. Technol.*, 36(8–9), 7–12.

Georgakakos, K. P. (1996). "A generalized stochastic hydrometeorological model for flood and flash-flood forecasting. 2: Case studies." *Water Resour. Res.*, 22(13), 2096–2106.

Giuliani, S., Hamouda, A., Mourot, G., Boukhris, A., and Auchel, P. (1996). "Rainfall measurement from tipping bucket rain gauges: Evaluation of uncertainties and gauge calibration." *Proc., 7th Int. Conf. on Urban Storm Drainage (ICUSD)*, 103–108.

Habib, E., Krajewski, W. F., and Kruger, A. (2001). "Sampling errors of tipping-bucket rain gauge measurements." *J. Hydrol. Eng.*, 6(2), 159–166.

Habib, E., Krajewski, W. F., Nespor, V., and Kruger, A. (1999). "Numerical simulation studies of rain-gage data correction due to wind effect." *J. Geophys. Res.*, 104, 19723–19733.

Habib, E., and Meselhe, E. A. (2006). "Stage-discharge relations for low-gradient tidal streams using data-driven models." *J. Hydraul. Eng.*, 132(5), 482–492.

Humphrey, M. D., Istok, J. D., Lee, J. Y., Hevesi, J. A., and Flint, A. L. (1997). "A new method for automated dynamic calibration of tipping-bucket rain gauges." *J. Atmos. Ocean. Technol.*, 14, 1513–1519.

Klemes, V. (1986). "Operational testing of hydrological simulation models." *J. Hydrol. Sci.*, 31(1), 13–24.

Krajewski, W. F., Ciach, G. J., and Habib, E. (2003). "An analysis of small-scale rainfall variability in different climatological regimes." *Hydrol. Sci. J.*, 48, 151–162.

Downloaded 26 Nov 2008 to 128.255.27.170. Redistribution subject to ASCE license or copyright; see http://pubs.asce.org/copyright

Krajewski, W. F., Lakshmi, V., Georgakakos, K. P., and Jain, S. C. (1991). "A Monte Carlo study of rainfall sampling effect on a distributed catchment model." *Water Resour. Res.*, 27(1), 119–128.

Legates, D. R., and Deliberty, T. L. (1993). "Precipitation measurement biases in the United States." *Water Resour. Bull.*, 29, 855–861.

Luyckx, G., and Berlamont, J. (2001). "Simplified method to correct rainfall measurements from tipping bucket rain gauges." *Proc., Urban Drainage Modeling*, ASCE, 767–776.

Monteith, J. L. (1965). "Evaporation and environment." *Proc., Symp. Society of Experimental Biology*, XIX, 205–234.

Neary, V., Habib, E., and Fleming, M. (2004). "Hydrologic modeling with NEXRAD precipitation in middle Tennessee." *J. Hydrol. Eng.*, 9(5), 339–349.

Nespor, V., and Sevruk, B. (1999). "Estimation of wind-induced error of rainfall gauge measurements using a numerical simulation." *J. Atmos. Ocean. Technol.*, 16, 450–464.

Niemczynowicz, J. (1986). "The dynamic calibration of tipping-bucket raingauges." *Nord. Hydrol.*, 17, 203–214.

Nystuen, J. A., and Proni, J. R. (1996). "A comparison of automatic rain gauges." *J. Atmos. Ocean. Technol.*, 13, 62–73.

Ogden, F. L., and Saghafian, B. (1997). "Green and Ampt infiltration with redistribution." *J. Irrig. Drain. Eng.*, 123(5), 386–393.

Schilling, W. (1991). "Rainfall data for urban hydrology: What do we need?" *Atmos. Res.*, 27, 5–21.

Sevruk, B., and Hamon, W. R. (1984). "International comparison of national precipitation gauges with a reference pit gauge, instruments, and observing methods." *Rep. No. 17*, World Meteorological Organization, Geneva.

Sevruk, B., and Lapin, M. (1993). "Precipitation measurement and quality control." *Proc., Int. Symp. on Precipitation and Evaporation*, *Bratislava*, Vol. 1, Slovak Hydrometeorological Institute, 207.

Sun, S., Mein, R. G., Keenan, T. D., and Elliott, J. F. (2000). "Flood estimation using radar and raingauge data." *J. Hydrol.*, 239, 4–18.

Yang, D., Goodisson, B. E., and Metcalfe, J. R. (1998). "Accuracy of NWS 8 standard nonrecording precipitation gauge: Results and application of WMO intercomparison." *J. Atmos. Ocean. Technol.*, 1(3), 241–254.

Yu, B., Ciesiolka, C. A. A., Rose, C. W., and Coughlan, K. J. (1997). "A note on sampling errors in the rainfall and runoff data collected using tipping bucket technology." *Trans. ASAE*, 40(5), 1305–1309.

Zhu, H.-J., and Schilling, W. (1996). "Simulation errors due to insufficient temporal rainfall resolution-annual combined sewer overflow." *Atmos. Res.*, 42, 19–32.

Downloaded 26 Nov 2008 to 128.255.27.170. Redistribution subject to ASCE license or copyright; see http://pubs.asce.org/copyright